Crystallization kinetics of sputter-deposited amorphous AgInSbTe films

Walter K. Njoroge, and Matthias Wuttig

Citation: Journal of Applied Physics **90**, 3816 (2001); doi: 10.1063/1.1405141
View online: https://doi.org/10.1063/1.1405141
View Table of Contents: http://aip.scitation.org/toc/jap/90/8
Published by the American Institute of Physics

Crystallization kinetics of sputter-deposited amorphous AgInSbTe films

Walter K. Njoroge
I. Physikalisches Institut der RWTH Aachen, D-52056 Aachen, Germany and Department of Physics, Kenyatta University, P.O. Box 43844 Nairobi, Kenya

Matthias Wuttig[a)]
I. Physikalisches Institut der RWTH Aachen, D-52056 Aachen, Germany and ISG3, Forschungszentrum Jülich, D-52428 Jülich, Germany

(Received 20 March 2001; accepted for publication 26 July 2001)

AgInSbTe films have recently attracted considerable interest as advanced materials for phase change recording. For this application the determination of crystallization kinetics is of crucial importance. In this work the temperature dependence of structural and electrical properties of sputtered AgInSbTe films has been determined. Temperature dependent measurements of the electrical resistance have been employed to study the kinetics of structural changes of these films. Upon annealing a major resistivity drop is observed at around 160 °C which can be attributed to a structural change as corroborated by x-ray diffraction. X-ray diffraction shows an amorphous phase for as-deposited films, while crystalline films with hexagonal structure ($a=4283$ Å, $c=16\,995$ Å) are obtained upon annealing above 160 °C. By applying Kissinger's method, an activation energy of 3.03 ± 0.17 eV is obtained for the crystallization. X-ray reflection measurements reveal a density increase of $5.2\%\pm0.2\%$ and a thickness decrease of $5.5\%\pm0.2\%$ upon crystallization. © *2001 American Institute of Physics.* [DOI: 10.1063/1.1405141]

I. INTRODUCTION

Materials which can be stabilized in two different physical states that exhibit significantly different optical properties have attracted much interest in recent years due to their potential application in phase change media technology. These materials are used as the memory device in rewritable phase change optical disks.[1–3] The key attributes for promising rewritable storage media include high-speed writing and erasing, adequate number of overwrite cycles, stable marks, sufficiently high signal-to-noise ratio, and good recording sensitivity.[4] Currently applied phase change media are mainly based on two families of phase change materials, namely ternary Ge:Sb:Te alloys or quaternary Ag:In:Sb:Te alloys. Several ternary stoichiometric alloys formed with compositions along the $GeTe–Sb_2Te_3$ line[5] have been identified as possible candidates for use in erasable disks. Among these alloys are $GeSb_4Te_7$, $GeSb_2Te_4$ and $Ge_2Sb_2Te_5$. Most studies have been focused on $Ge_2Sb_2Te_5$[6–10] due to its excellent properties regarding the reflectivity change between the amorphous and crystalline state, its cyclability of recording and erasing, and also its durability at room temperature. Recently, in order to improve the stability of amorphous marks at high temperature and also to increase the density of the marks, a new alloy has been developed based on AgInSbTe.[11] A high density of 12 GB capacity and a high data-transfer rate of 30 Mbps corresponding to that of a DVD-ROM have been reported using an AgInSbTe phase change material.[12] Despite the technological use of this material, very little information has been reported on its properties. Iwasaki *et al.*[13] have reported on the structural changes of $Ag_{0.08}In_{0.13}Sb_{0.49}Te_{0.30}$. Structural properties of vanadium doped AgInSbTe films have also been reported by Duc *et al.*[14] and Tominaga *et al.*[11,15]

The determination of crystallization kinetics and the underlying mechanisms is of crucial importance for the performance of the material. In addition, it provides useful information to improve the switching behavior and enables a higher rate of data transfer and the development of new materials with superior properties. In this work we report on the temperature dependence of structural and electrical properties of sputtered AgInSbTe films. Temperature dependent measurements of the electrical resistance have been employed to study the kinetics of structural changes of these films. X-ray reflectivity measurements (XRR) are used to determine the temperature dependence of thickness, roughness and the density of the films. The temperature dependence of the film structure is determined by x-ray diffraction (XRD). In the next section, the experimental procedures are discussed while the results are presented and discussed in the third section. A short summary is presented in Sec. IV.

II. EXPERIMENTAL PROCEDURES

AgInSbTe films with thickness between 40 and 200 nm were deposited on glass or silicon substrates at room temperature by dc magnetron sputtering. The composition of the sputtered film was determined by energy dispersive x-ray analysis to $Ag_5In_6Sb_{59}Te_{30}$. The background pressure of the sputter system was 2×10^{-7} mbar. An Ar pressure of 7.5×10^{-3} mbar and a power of 100 W were used to deposit the films. The resulting growth rate was determined to be 0.5 nm/s. XRR measurements were performed to determine the thickness, roughness and the density of the films while XRD

a)Electronic mail: wuttig@physik.rwth-aachen.de

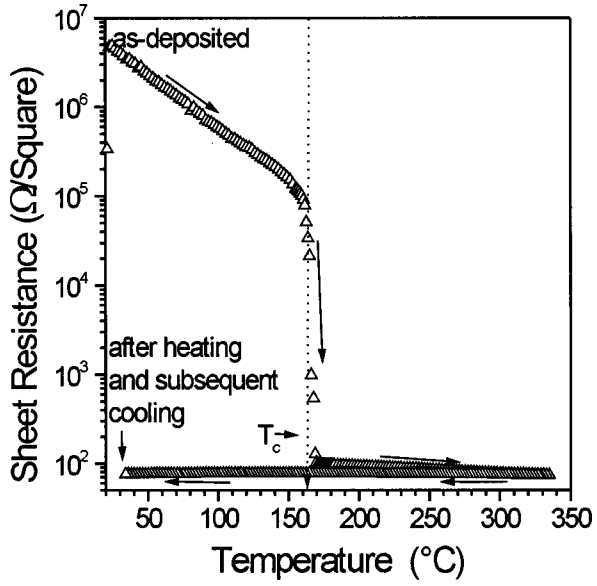

FIG. 1. Temperature dependence of the sheet resistance R_s for a 100 nm thin film (heating rate $(dT/dt)=3$ K/min). The dotted line denotes the transition temperature T_c.

measurements were used to determine the structure. These measurements were carried out using a Philips X'pert materials research diffractometer (MRD) system. The system is equipped with a knife edge which is placed above the sample surface when measuring XRR of films deposited on slightly curved substrates. The divergence of the x-ray beam was set to 1/64° and a detector slit of 0.1 mm was used for XRR measurements. A grazing angle geometry ($\theta=0.75°$) was preferred for XRD measurement since this arrangement improves the signal-to-noise ratio for very thin films. Films of 45 and 200 nm were used for XRR and XRD characterization, respectively. All measurements were performed at room temperature.

The sheet resistance was measured with a four-point probe setup following the procedure proposed by van der Pauw.[16] The setup allows us to monitor the sheet resistance upon annealing in argon ambient. The sample temperature was measured by a NiCr–Ni thermocouple.

III. RESULTS AND DISCUSSION

A. Resistance dependence on temperature

Figure 1 displays a typical dependence of the sheet resistance R_s upon the temperature of a 100 nm thin film obtained using a heating rate of 3 K/min. As-deposited films have a sheet resistance of 6 MΩ/□ which corresponds to a resistivity ρ of 60 Ω cm. A continuous decrease in sheet resistance upon annealing is observed below a temperature T_c where a sudden drop occurs. It drops to a value of 100 Ω/□ ($\rho=10^{-3}$ Ω cm). Further annealing only reduces the sheet resistance slightly. On cooling to room temperature a further slight reduction in sheet resistance is noted. The sudden drop in sheet resistance at T_c can only be explained by a change in the physical state which is accompanied by a pronounced change in electronic structure. To confirm that this change is due to a transformation in physical state, the structure of various films has been analyzed after annealing them at different temperatures in argon ambient.

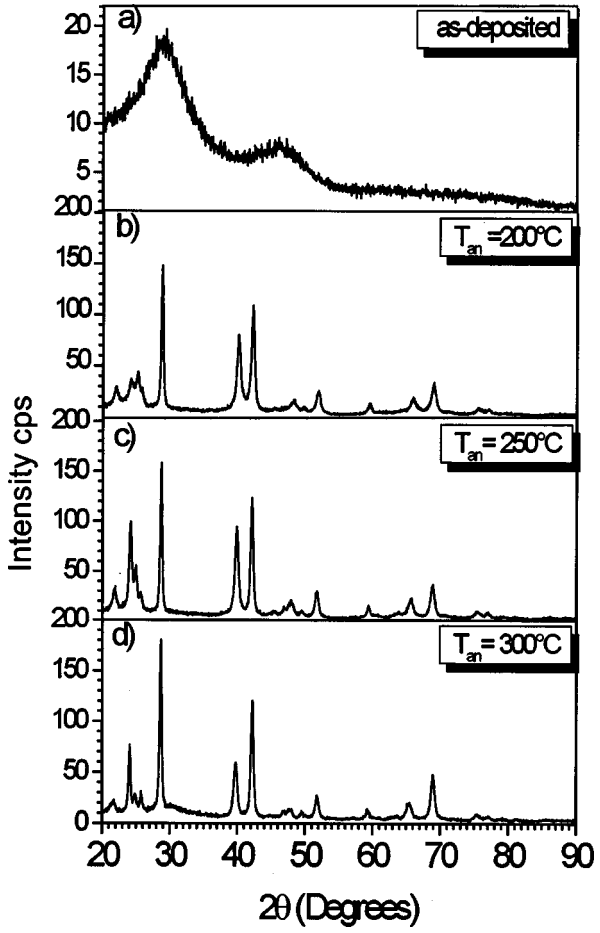

FIG. 2. X-ray diffraction scans of 200 nm AgInSbTe films on a glass substrate after annealing at different temperatures. All measurements were performed under a grazing angle θ of 0.75° (a) as-deposited sample. (b) Annealed at 200 °C for 5 h. (c) Annealed at 250 °C for 5 h. (d) Annealed at 300 °C for 5 h.

B. Film structure dependence on temperature

Figure 2 shows XRD scans performed on samples annealed isothermally at different temperatures. In each case, a 200 nm thin film was annealed for 5 h. Figure 2(a) shows the XRD pattern of the as-deposited sample. The two broad peaks confirm a disordered phase for the as-deposited AgInSbTe films. Figures 2(b)–2(d) show XRD patterns of samples annealed at 200, 250 and 300 °C, respectively. Diffraction peaks, indicative for a crystalline phase, are observed in all three patterns. This confirms that the resistivity drop at T_c is caused by the phase transition from an amorphous to a crystalline phase. The three diffraction patterns are very similar implying that there is no further structural change in the temperature range from 200 to 300 °C.

XRD scans (not shown here) performed on samples annealed at temperatures between 170 and 380 °C all show very similar spectra. The only notable differences are the peak intensities for small diffraction angles and the development of the peak width. The peaks become slightly sharper

TABLE I. The observed and calculated peak positions for the spectra shown in Figs. 2(b)–2(d). The lattice parameters deduced from these values are ($a=4.283\pm0.001$ Å, $c=16.995\pm0.018$ Å), ($a=4.288\pm0.001$ Å, $c=17.085\pm0.004$ Å) and ($a=4.289\pm0.001$ Å, $c=17.162\pm0.018$ Å) for the samples annealed at 200, 250 and 300 °C, respectively.

Observed (Ob.) and Calculated (Cal.) Peak positions ($2\theta°$)						
Peak (hkl)	200 °C Ob.	200 °C Cal.	250 °C Ob.	250 °C Cal.	300 °C Ob.	300 °C Cal.
1 0 0	24.090	23.970	24.087	23.940	24.068	24.005
1 0 1	24.770	24.540	24.876	24.51	24.853	24.557
0 0 5	25.914	26.190	25.850	26.060	25.768	25.707
1 0 3	28.756	28.745	28.677	28.676	28.662	28.613
1 0 6	40.096	40.019	39.862	39.864	39.748	39.558
1 1 0	42.181	42.163	42.112	42.115	42.230	42.224
2 0 3	51.885	51.829	51.736	51.746	51.797	51.801
2 0 6	59.425	59.531	59.393	59.378	59.207	59.236
1 1 9	65.911	65.894	65.638	65.639	65.178	65.175
2 1 3	68.941	68.946	68.827	68.841	68.974	68.966
2 1 6	75.617	75.622	75.449	75.453	75.269	75.402
3 0 0	77.086	77.072	76.985	76.985	77.276	77.199

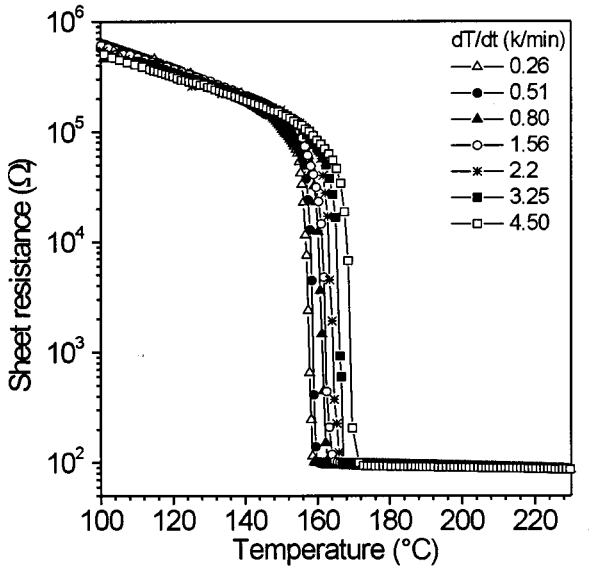

FIG. 3. Temperature dependence of the sheet resistance R_s for 100 nm AgInSbTe films measured with different heating rates (dT/dt). The heating rates are shown in the inset.

as the annealing temperature increases. This can be explained as a result of grain growth and explains the slight reduction in sheet resistance after the transition. The spectra can be identified with a hexagonal structure similar to that of Sb_2Te[17] with lattice parameters of $a=4.283\pm0.001$ Å and $c=16.995\pm0.018$ Å for the sample annealed at 200 °C. The observed and calculated peak positions for the spectra shown in Figs. 2(b)–2(d) are tabulated in Table I. A slight increase in the lattice parameters is observed with increasing annealing temperature, from $a=4.288\pm0.001$ Å and $c=17.085\pm0.004$ Å at 250 °C to $a=4.289\pm0.001$ Å and $c=17.162\pm0.018$ Å at 300 °C. It is interesting to note that these values are similar to the values reported by Friedrich *et al.*[6] and Petrov, Imamov, and Pinsker[18] for the hexagonal phase of $Ge_2Sb_2Te_5$. They reported values of $a=4.22\pm0.008$ Å, $c=17.18\pm0.04$ Å and $a=4.2\pm0.02$ Å, $c=16.96\pm0.06$ Å, respectively. Unfortunately, it is impossible to determine the precise atomic positions within the unit cell since the atomic form factors of the four atomic species (Ag, In, Sb, Te) only differ by a very small amount. Nevertheless, it is reasonable to assume that nine atoms occupy the unit cell. Taking into account the measured film stoichiometry ($Ag_5In_6Sb_{59}Te_{30}$), this leads to an x-ray density of 6.7 g/cm^3.

Earlier studies of the structure of AgInSbTe films have often reported a mixture of phases.[13,14] Iwasaki *et al.*[13] investigated the structural changes of $Ag_{0.08}In_{0.13}Sb_{0.49}Te_{0.30}$ films prepared by conventional rf sputtering using an $AgInTe_2$ target cosputtered with Sb chips. Crystalline $AgInTe_2$ plus crystalline Sb was obtained for low-power laser annealing while crystalline $AgSbTe_2$ plus amorphous In–Sb resulted from higher power laser annealing. Duc *et al.*[14] have shown that there exist at least three crystalline phases for vanadium doped AgInSbTe alloys with Sb and $AgSbTe_2$ being the main phases. Tominaga *et al.*[11] have also investigated vanadium doped AgInSbTe films and found a single crystalline phase which they identified as $AgSbTe_2$ with an excess of Sb.

C. Kinetics of the structural transformation

Now that XRD has established the irreversible structural change at T_c, we use resistance measurements to determine the activation barrier for crystallization. In Fig. 3 the temperature dependence of sheet resistance obtained using different heating rates (dT/dt) is shown. The heating rates are indicated in the inset for each curve. The sudden drop in the sheet resistance is observed in the range from 155 to 170 °C. A shift in the position of the steep decline in the sheet resistance and therefore a shift in the phase transformation to higher temperatures with increasing heating rate is clearly visible. Such measurements allow the determination of the activation energy E_a of the transformation. We apply Kissinger's[19] analysis which relates the transition temperature T_c, the rate of heating (dT/dt), and the activation energy E_a by the formula

$$\ln[(dT/dt)/T_c^2]=C+(E_a/k_BT_c) \tag{1}$$

where C is a constant and k_B is the Boltzmann constant. A plot of $\ln[(dT/dt)/T_c^2]$ against $1/T_c$ will yield a straight line with slope E_a/k_B.

From the sheet resistance measurements we determine T_c for different heating rates dT/dt by locating the minimum in the first derivative (dR_s/dT). The activation energy is determined from the corresponding Kissinger plot, shown in Fig. 4 to be 3.03 ± 0.17 eV. The activation energy is higher than the value obtained by other groups[6,7,20] for the crystallization of $Ge_2Sb_2Te_5$ films, implying a higher stability against recrystallization. However, it should be noted that the activation energy depends to some extent on the method of analysis employed. It has been shown that a nonisothermal method usually yields higher activation energies as compared to the isothermal method.[21,22] In the case of the isothermal method, the samples are initially heated at a very high rate to reach the desired annealing temperature. It is likely that a small but finite number of nuclei are precipitated

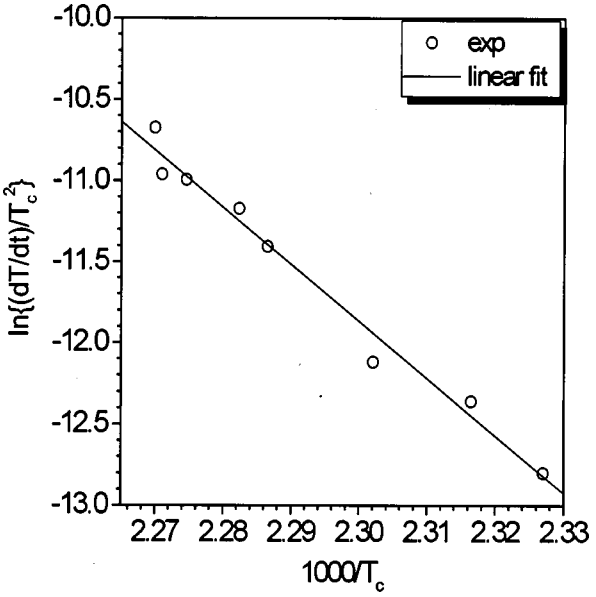

FIG. 4. Kissinger plot from which the activation energy E_a of the amorphous to crystalline transition at T_c is determined (100 nm AgInSbTe films were used).

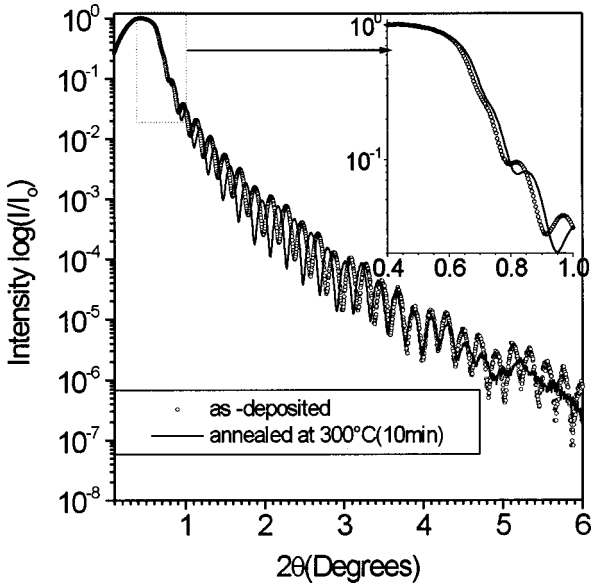

FIG. 5. X-ray reflection measurement of an as-deposited sample (solid circles) and x-ray reflection measurement of the same sample after annealing at 300 °C for 10 min (open circles). The inset shows the area around the total reflection edge.

on the surface and in the sample. This results in lowering of the energy barriers separating the metastable and stable phases. Thus, on the average, the barriers experienced by the diffusing atoms are reduced and this is reflected in the calculated activation energy.

D. Temperature dependence of density

Besides the activation energy, another quantity which is important for the application of chalcogenide films in optical storage media is the film density. The density changes upon crystallization and this leads to considerable stresses which can limit the lifetime of storage media. This density change can be determined from x-ray reflection measurements. Figure 5 depicts x-ray reflection measurements of an as-deposited sample and an XRR measurement of the same sample after annealing at 300 °C for 10 min. The inset shows the area around the total reflection edge. One observes a shift in the total reflection edge towards higher angles. Hence it can be concluded that the as-deposited sample has a lower density than the annealed sample since the density (ϱ) is directly proportional to the square of the critical angle (θ_c) as it can be derived from the following equation:

$$\theta_c = \lambda \sqrt{\frac{N_A r_0}{\pi} \frac{\varrho}{A} (f_0 + f')}, \tag{2}$$

where N_A, r_0, λ, A and $(f_0 + f')$ are the Avogadro constant, Bohr radius, wavelength of the used x rays, atomic mass and the atomic form factor, respectively.

Another notable feature is the decay of the oscillation amplitude, especially at higher angles. The oscillations of the as-deposited sample are clearly visible in the whole angular range while the oscillations of the annealed sample tend to decrease more strongly for larger angles. The decay in the oscillations is related to the roughness of the sample. With increasing roughness, a faster decay in the oscillation amplitude is expected. Hence this is an indication for an increase in roughness upon annealing.

Figure 6 shows the spectra displayed in Fig. 5 plus the corresponding theoretical simulations. A spectrum of the same sample annealed at 180 °C has also been added. Densities of 6.27 ± 0.05, 6.57 ± 0.05 and 6.59 ± 0.05 g/cm^3 are obtained for the as-deposited sample, annealed at 180 and 300 °C, respectively. The corresponding roughness values are 0.01, 0.15 and 0.34 nm, respectively. These values show an increase in roughness upon crystallization as expected. However, the highest value is still below 5 Å. Therefore we can conclude that thermal annealing will not degrade the interface quality when these films are applied as active layers in phase change media. The increase in density and roughness upon annealing is therefore confirmed by the values derived from the simulation. The film density measured by XRR for films annealed above T_c closely resembles the crystalline density measured by XRD ($\delta_{\mathrm{XRD}} = 6.7$ g/cm^3). This implies that the films are nearly void free. More XRR measurements (not shown here) were performed for samples annealed at different temperatures and the results are displayed in Fig. 7. The density remains constant with an average value of 6.26 ± 0.05 g/cm^3 up to T_c where an abrupt increase to 6.59 ± 0.05 g/cm^3 is observed. This corresponds to an increase of 5.2% in the density. There is no evidence of any density change at higher temperatures up to 320 °C. This confirms that the material stabilizes in one crystalline structure only. This is an advantage over $Ge_2Sb_2Te_5$ which has two different crystalline structures with different density. Figure 8 shows the normalized thickness versus temperature. Two segments with constant value are clearly visible. Upon annealing above 150 °C a decrease of 5.5% in the thickness is measured. This correlates very well with the increase in the density of 5.2% illustrated by Fig. 7, implying that there

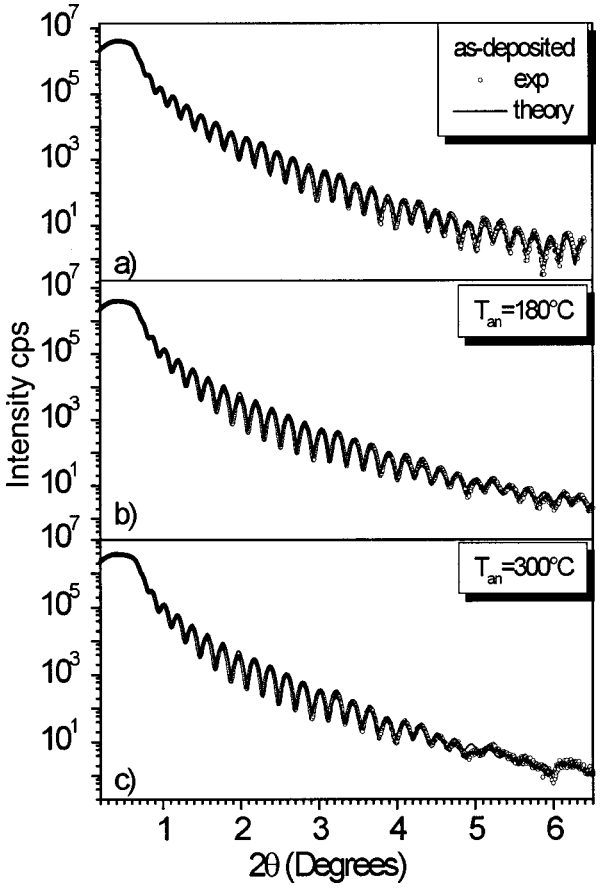

FIG. 6. X-ray reflection measurements plus the corresponding theoretical simulation of a sample (a) as-deposited, (b) after annealing at 180 °C for 10 min and (c) after annealing at 300 °C for 10 min.

is no loss of material during the phase transformation. The density change and the corresponding thickness (volume) change are slightly lower than the values reported by Weidenhof *et al.*[8] for the $Ge_2Sb_2Te_5$ material which are an increase of $6.2\% \pm 0.8\%$ and reduction of $6.0\% \pm 0.6\%$, respectively. Therefore, the stresses which accompany the phase transformation should be smaller for AgInSbTe than for $Ge_2Sb_2Te_5$. As a consequence, AgInSbTe could allow a higher number of overwrite cycles than $Ge_2Sb_2Te_5$ if mechanical stresses determine the cyclability.

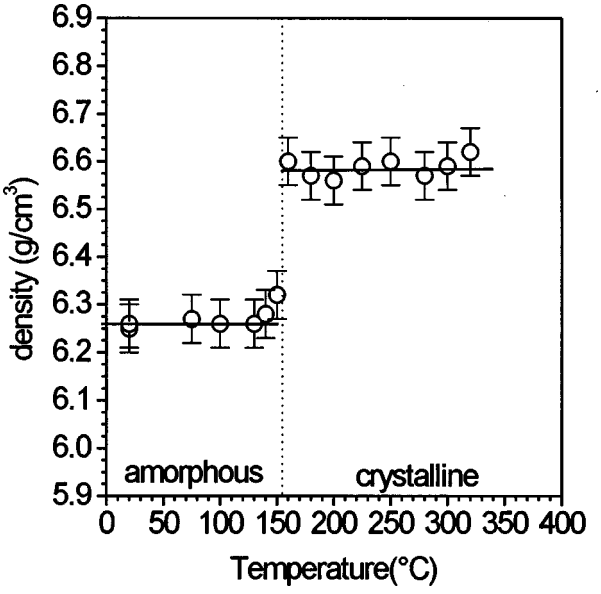

FIG. 7. Temperature dependence of the density for AgInSbTe films obtained from XRR measurements.

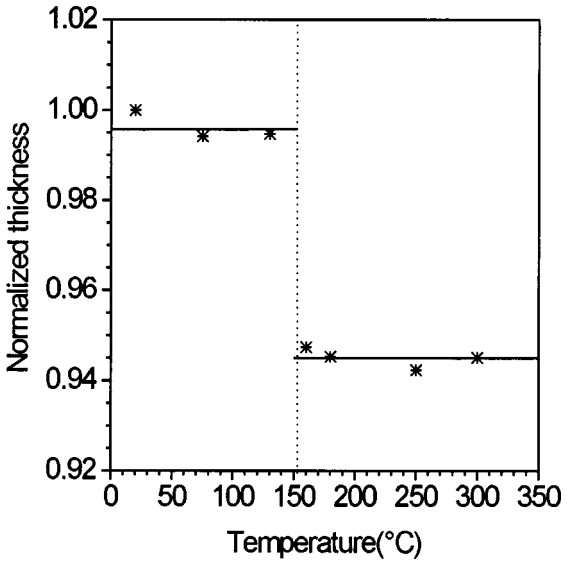

FIG. 8. Normalized thickness variation with temperature for AgInSbTe films obtained from XRR measurements.

IV. CONCLUSION

We have investigated the temperature dependence of structural and electrical properties of sputtered AgInSbTe films. The as-deposited state is amorphous with a resistivity of $\rho = 60\ \Omega\,\mathrm{cm}$ and a density of $6.26 \pm 0.02\ \mathrm{g/cm^3}$. Upon annealing above 150 °C, the films rapidly crystallize in a hexagonal structure similar to that of Sb_2Te. The lattice parameters increase slightly upon annealing at higher temperatures. Values of ($a = 4.283 \pm 0.001$ Å, $c = 16.995 \pm 0.018$ Å), ($a = 4.288 \pm 0.001$ Å, $c = 17.085 \pm 0.004$ Å) and ($a = 4.289 \pm 0.001$ Å, $c = 17.162 \pm 0.018$ Å) are obtained for samples annealed at 200, 250 and 300 °C, respectively. The density and resistivity of the crystalline state are $6.59 \pm 0.02\ \mathrm{g/cm^3}$ and $10^{-3}\ \Omega\,\mathrm{cm}$, respectively. A thickness (volume) decrease of $5.5\% \pm 0.2\%$ is calculated for the phase transition (amorphous-crystalline) which agrees quite well with the density increase which is $5.2\% \pm 0.2\%$. By applying Kissinger's method, the activation energy for the phase transformation is determined to be 3.03 ± 0.17 eV.

ACKNOWLEDGMENTS

The authors are grateful to M. Gartz of Steag Eta-Optik for fruitful discussions. One of the authors (W. K. Njoroge) would like to thank the DAAD for a scholarship. The Ministerium für Schule, Weiterbildung, Wissenschaft und Forschung des Landes Nordrhein-Westfalen is gratefully acknowledged for the financial support.

[1] J. Feinleib, J. de Neufville, S. C. Moss, and S. R. Ovshinsky, Appl. Phys. Lett. **18**, 254 (1971).
[2] N. Akahira, N. Miyagaya, K. Nishiuchi, Y. Sakawe, and E. Ohono, Proc. SPIE **2514**, 294 (1995).
[3] N. Nobukuni, M. Takashima, T. Ohono, and M. Horie, J. Appl. Phys. **78**, 6980 (1995).
[4] Y. Kim Sang, J. Kim Sang, H. Seo, and M. R. Kim, Jpn. J. Appl. Phys., Part 1 **38**, 1713 (1999).
[5] N. Ohshima, J. Appl. Phys. **79**, 8357 (1996).
[6] I. Friedrich, V. Weidenhof, W. Njoroge, P. Franz, and M. Wuttig, J. Appl. Phys. **87**, 4130 (2000).
[7] J. Park, M. R. Kim, W. S. Choi, H. Seo, and C. Yeon, Jpn. J. Appl. Phys., Part 1 **38**, 4775 (1999).
[8] V. Weidenhof, I. Friedrich, S. Ziegler, and M. Wuttig, J. Appl. Phys. **86**, 5879 (1999).
[9] J. H. Kim, J. Appl. Phys. **86**, 6770 (1999).
[10] J. Tominaga, T. Nakano, and N. Atoda, Jpn. J. Appl. Phys., Part 1 **387**, 1852 (1998).
[11] J. Tominaga, T. Kikukawa, M. Takahashi, and R. T. Phillips, J. Appl. Phys. **82**, 3214 (1997).
[12] M. Shinotsuka, N. Onagi, and M. Harigaya, Jpn. J. Appl. Phys., Part 1 **39**, 976 (2000).
[13] H. Iwasaki, M. Harigaya, O. Nonoyama, Y. Kageyama, M. Takahashi, K. Yamada, H. Deguchi, and Y. Ide, J. Appl. Phys. **32**, 5241 (1993).
[14] I. Duc, P. Hancock, J. Tominaga, R. Inaba, and S. Haratani: Extended Abstract (42nd Spring Meeting, 28–31 March, 1995), The Japan Society of Applied Physics and Related Societies, Kanagawa, Japan, 28pT-10 (unpublished).
[15] J. Tominaga, T. Kikukawa, M. Takahashi, and T. Kato, Jpn. J. Appl. Phys., Part 1 **36**, 3598 (1997).
[16] L. J. van der Pauw, Philips Res. Rep. **13**, 1 (1958).
[17] JCPDS (80-1722).
[18] I. Petrov, R. M. Imamov, and Z. G. Pinsker, Sov. Phys. Crystallogr. **13**, 339 (1968).
[19] H. E. Kissinger, Anal. Chem. **29**, 1702 (1957).
[20] N. Yamanda, E. Ohono, K. Nishiuchi, N. Akahira, and M. Takao, J. Appl. Phys. **69**, 2849 (1991).
[21] K. Cheng, J. Mater. Sci. **36**, 1043 (2001).
[22] A. Nazareth and G. C. Hadjipanayis, Phys. Rev. B **40**, 5441 (1989).